Light Emission Probing Quantum Shot Noise and Charge Fluctuations at a Biased Molecular Junction

N. L. Schneider,[1] J. T. Lü,[2] M. Brandbyge,[2] and R. Berndt[1]

[1]*Institut für Experimentelle und Angewandte Physik, Christian-Albrechts-Universität zu Kiel, D-24098 Kiel, Germany*

[2]*DTU Nanotech, Technical University of Denmark, DK-2800 Kongens Lyngby, Denmark*

(Received 24 July 2012; published 31 October 2012)

The emission of plasmonic light from a single C_{60} molecule on Cu(111) is probed in a scanning tunneling microscope from the weak-coupling, tunneling range to strong coupling of the molecule to the electrodes at contact. At positive sample voltage the photon yield decreases owing to shot-noise suppression in an increasingly transparent quantum contact. At reversed bias an unexpected nonlinear increase occurs. First-principles transport calculations reveal that ultrafast charge fluctuations on the molecule give rise to additional noise at optical frequencies beyond the shot noise of the current that is injected to the tip.

DOI: 10.1103/PhysRevLett.109.186601 PACS numbers: 72.70.+m, 68.37.Ef, 73.20.Mf, 73.63.Rt

The interaction of light and molecular junctions between metallic surfaces is an important and challenging topic bridging nanoelectronics and plasmonics [1]. To probe the conductance of a single molecule it has to be contacted by two metallic leads. A side effect of the atomic-scale proximity of the leads is that electromagnetic coupling occurs between them. When noble metals are used, strong localized plasmon modes form, which in turn may interact with the molecule as well as with electrons traversing the junction. The scanning tunneling microscope (STM) has been used to investigate the emission of light from such junctions in the limit of weak coupling of the tip to the molecule. Molecules have been shown to modify the emission through fluorescence [2–6], via their effects on the plasmon modes [7–10], and via the density of final states for inelastic electron tunneling [2,11]. The strong coupling limit, where a quantum contact is formed, has recently been probed for contacts to single atoms [12,13]. The light emission has been found to reflect a suppression of the shot noise at optical frequencies, which drives the plasmons of the nanoscale junction [13]. Reduced noise is typical of uncorrelated transport and was previously observed at low frequencies [14–18]. Coulomb repulsion and charging effects, however, were suggested to significantly enhance current fluctuations [19–22].

Here we report the first investigation of light emission from a single molecule junction in the limit of strong coupling. This work was motivated by the possibility of using the optically detected shot-noise characteristics to disentangle the relative contributions of different transport channels to the conductance. To this end the tip of a low-temperature STM was controllably approached towards an oriented C_{60} molecule and the intensity of emitted light was monitored. A monotonic decrease of the light intensity was expected to occur as the relevant transport channels become more transparent at close tip-molecule distances. While such an effect is indeed observed when electrons move from the tip to the molecule, a strikingly different variation occurs at reversed bias. The light intensity initially increases drastically as the molecule is being contacted.

We analyzed the results with the help of first-principles calculations and found that charge fluctuations on the molecule occur, which enhance the current noise and thus the light emission. The fluctuations reflect the fact that electrons may spend time on the molecule while traversing the contact [23]. This is different from the case of a pure metal junction where the transport involves broad electronic resonances that correspond to short electron traversal times through the contact and strong delocalization of the electronic states.

The experiments were performed with an ultrahigh vacuum STM at low temperature (5.8 K). Light emitted from the junction was collected with a lens and guided to a grating spectrometer and a liquid nitrogen cooled CCD camera via an optical fiber. Spectra are not corrected for the detection efficiency, which was reported in Ref. [24]. Cu(111) surfaces and chemically etched W tips were cleaned *in vacuo* by Ar^+ bombardment and annealing. To increase the plasmon enhancement at the tip-sample junction, the tips were coated with Cu by indenting them into the sample. As the last step of preparation the tips were repeatedly brought closer to the sample at voltages $V = 1.3, \ldots, 2.0$ V, which was found to increase the stability of the tips during contact experiments.

After a deposition of C_{60} from a heated Ta crucible, the Cu(111) sample was annealed to ≈ 500 K. This leads to the formation of a well ordered C_{60} monolayer on a reconstructed Cu(111) surface [Fig. 1(a)] [25]. Most molecules are adsorbed with a C hexagon and give rise to a three-lobe pattern. dI/dV spectra of the molecules [Fig. 1(b)] show the characteristic features of C_{60} on reconstructed Cu(111), a lowest unoccupied molecular orbital (LUMO) straddling the Fermi energy, a highest occupied molecular orbital

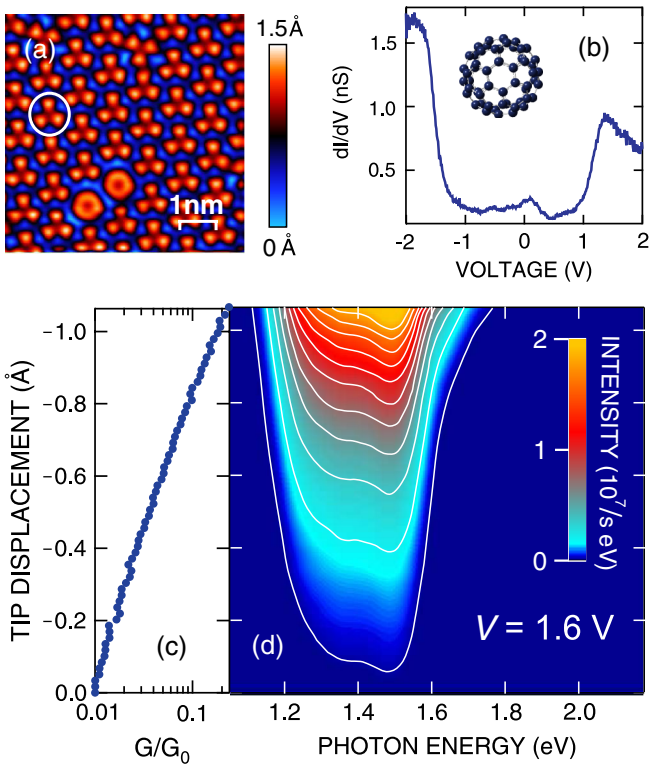

FIG. 1 (color online). (a) Constant-current STM image of a C_{60} monolayer on Cu(111). The white circle indicates a molecule adsorbed with a carbon hexagon. (b) Model of the molecule viewed from the STM tip (inset) and differential conductance (dI/dV) spectrum acquired with current feedback disabled over the molecule marked in (a). (c) Conductance in units of the conductance quantum $G_0 = 2e^2/h$ recorded during stepwise tip displacement from the tunneling range towards contact at $V = 1.6$ V. (d) Series of luminescence spectra recorded simultaneously with (c). Intensities are represented by false colors. Contour lines correspond to multiples of 1.8×10^6 s^{-1} eV^{-1}.

(HOMO) at $V \approx -1.85$ V, and a LUMO + 1 at 1.4 V, which is down-shifted compared to the unreconstructed surface [25]. Contacts to these molecules are stable up to $V \geq -1.7$ V and $I \leq 50$ μA.

The transition from tunneling to contact was probed by bringing the STM tip closer to the sample in 63 steps of ≈ 1.7 pm each at a rate of 2–10 steps per second. Constant-current images were recorded before and after contact experiments and the current was monitored to detect changes of tip or sample. All data presented here were recorded without any detected changes.

Figures 1(c) and 1(d) show the tip displacement versus the conductance $G = I/V$ at positive sample voltage $V = 1.6$ V along with a series of light emission spectra, which were recorded simultaneously. The data cover the range $G/G_0 = 0.01$–0.22. The highest conductances are close to those reported from contacts to C_{60} on Cu(111) at low bias [26]. At the high positive bias used here (1.3–1.6 V), further tip approach typically led to decomposition of the molecules [27]. The overall shape of the spectra reflects the tip-induced plasmon resonance of the junction [28]. The electronic states of the molecule, in particular the LUMO around the Fermi level, are involved in the process as they provide the final states for inelastic transitions [11], but they do not cause distinct features in the spectra. The emission at low conductances $G \lesssim 0.05G_0$ occurs at photon energies $h\nu < eV$ as expected for one-electron processes. At elevated conductances, emission at $h\nu > eV$ is also observed. It has been attributed to electrons which have been promoted to the energy levels above the Fermi energy via electron-electron scattering [12,29,30].

Figure 2 displays the conductance and a sequence of spectra acquired at $V = -1.7$ V. The conductance [Fig. 2(a)] exhibits a jump from tunneling to contact; however, no irreversible changes of the tip or sample occur. Spectra of the emission in the tunneling range [Fig. 2(b)] show low intensity. At the point of contact with the molecule, the intensity drastically increases. It reaches maximum in the contact range at a conductance of $\sim 0.2G_0$ and then decreases despite the continued increase of the current. In the contact range one- and two-electron components are clearly resolved in the spectra. Below we focus on single electron processes ($h\nu < eV$).

The photon yield, which we define as the intensity in the range $h\nu < eV$ per current and normalized to 1 at low conductances, is shown in Fig. 3. At $V > 0$, Fig. 3(a), the yield decreases monotonically. The variation is significantly different at negative bias. In the tunneling range at conductances $G > 0.015G_0$ the photon yield slightly increases. At the point of contact formation (arrow in Fig. 2), it abruptly rises by a factor of ≈ 2.5. Deeper in the contact range the yield decreases again with a change of slope at $0.25G_0$.

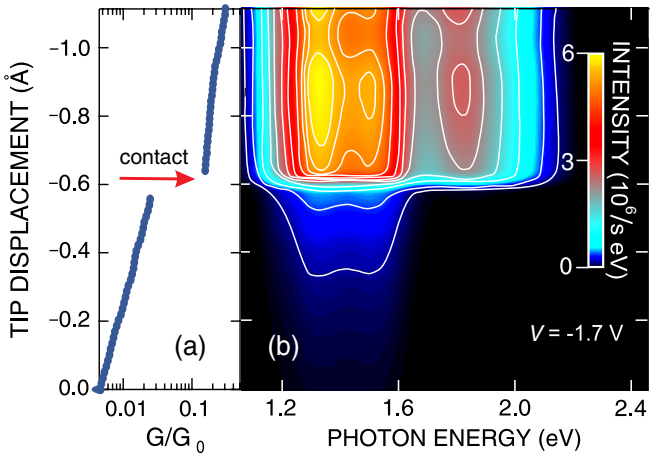

FIG. 2 (color online). (a) Tip displacement versus conductance from tunneling to contact at $V = -1.7$ V. (b) Series of luminescence spectra recorded simultaneously with (a). Contour lines correspond to multiples of 5×10^5 s^{-1} eV^{-1}. An abrupt transition to contact occurs at the tip displacement indicated by the arrow.

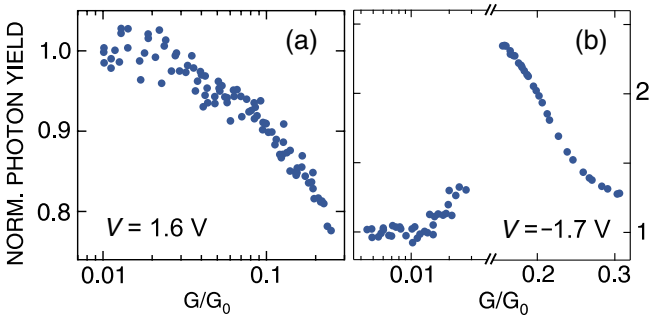

FIG. 3 (color online). Yield of photons with $1.22 < h\nu < 1.57$ eV and $1.21 < h\nu < 1.62$ eV versus conductance at (a) positive and (b) negative sample voltage V, respectively.

Below we show that the marked dependencies of the light emission on the conductance and on the bias polarity can be traced back to the nonequilibrium electronic structure of the molecular contact. We performed first-principles density functional theory (DFT) and nonequilibrium Green function (NEGF) calculations of the electronic structure and the conductance using the SIESTA/TRANSIESTA code [31,32]. Detailed information can be found in the Supplemental Material [33]. Five electrode separations covering the range from tunneling to contact were considered. The inset of Fig. 4(a) shows the relaxed geometry of the junction at the smallest electrode spacing. Following Refs. [34–36] we consider the plasmon excitation and resulting photon emission as a "measuring device" for the excess quantum noise generated by the current in the junction. Importantly, rather than using averaged currents in the electrodes far away from the junction [35], we consider the local currents between C_{60} and the electrodes. Previously only the current between tip and sample was used in the description of the tunneling regime [37]. Here, however, we define the C_{60} molecule as the device (d) and consider the local current injected into d from the sample $\hat{I}_s$ and from the tip $\hat{I}_t$. According to charge conservation, their sum $\hat{I}_d = \hat{I}_s + \hat{I}_t$ characterizes the fluctuations of the C_{60} charge Q_d,

$$\dot{\hat{Q}}_d = -\dot{\hat{Q}}_s - \dot{\hat{Q}}_t \equiv \hat{I}_s + \hat{I}_t. \tag{1}$$

In the limit of zero temperature ($k_B T \ll h\nu$), the excess shot noise with frequency ν is characterized by the current-current correlation function, $S_{\alpha\beta}(h\nu)$, $\alpha, \beta = s, t, d$. This can be written using the electrode scattering states ψ_t, ψ_s [34,35],

$$S_{\alpha\beta}(h\nu) = h \sum_{\substack{\varepsilon_s > \mu_s \\ \varepsilon_t < \mu_t}} \langle\psi_t|\hat{I}_\alpha|\psi_s\rangle\langle\psi_s|\hat{I}_\beta|\psi_t\rangle\delta(\varepsilon_t - \varepsilon_s - h\nu), \tag{2}$$

for positive sample bias $eV = \mu_t - \mu_s > 0$. s and t should be exchanged for $V < 0$.

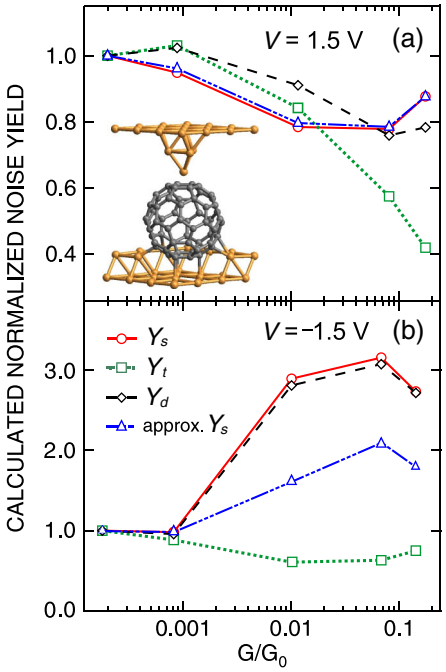

FIG. 4 (color online). Calculated zero-temperature noise yields $Y_\alpha = S_{\alpha\alpha}/I$, $\alpha = s, t, d$, normalized to 1 at low conductance as a function of average conductance from tunneling to contact. (a) Positive, (b) Negative sample bias. The approximate curve was obtained using Eqs. (3) and (4), and all others using Eq. (2). Lines serve to guide the eye. Inset of (a): Calculations were carried out for five tip-C_{60} distances. Here the relaxed geometry of the contact region at the smallest distance is displayed.

The "diagonal" correlations $S_{\alpha\alpha}$ are proportional to the emission rate of photons with energy $h\nu$ driven by the fluctuations of $\hat{I}_\alpha$ [34]. The noise $S_{\alpha\beta}$ and the currents can be obtained directly from the DFT-NEGF calculations (see the Supplemental Material [33]). Importantly, we can gain insight into which of the current fluctuations are most strongly coupled to the photon emission by comparing calculated and measured yields. Figure 4 shows the calculated normalized yield Y_α, which is defined as emission rate per dc current ($S_{\alpha\alpha}/I$), and normalized to 1 at low conductances, for the five electrode separations at $V = \pm 1.5$ V and $h\nu = 1.2$ eV. In the case $V > 0$, all calculated $S_{\alpha\alpha}$, $\alpha = s, t, d$, are similar in magnitude, and result in a slowly decreasing yield [Fig. 4(a)] with increasing conductance. This is in accordance with the experimental data of Fig. 3(a). For $V < 0$ [Fig. 4(b)], the calculated results are markedly different. The rates due to fluctuations of the molecular charge $\hat{I}_d$ and the sample-molecule current $\hat{I}_s$ are approximately 4 times larger than that due to $\hat{I}_t$, the fluctuation of the molecule-tip current. Moreover, they cause a strong increase of the emission as a contact is formed. This behavior closely resembles the experimental data of Fig. 3(b). We note that the atomic structure was

relaxed at zero bias and does not capture the abrupt jump-to-contact observed for $V < 0$.

In order to understand the trend of the yield with tip approach we derive approximate simplified expressions for S_{ss} and S_{tt} assuming wideband electrodes and uncoupled eigenchannels at different energies (cf. the Supplemental Material [33]). Denoting the channel transmissions at sample bias V by T_n, we get the approximations

$$S_{ss}^{>} \propto \sum_n \int_{-|eV|/2+h\nu}^{|eV|/2} T_n(\varepsilon)[1 - T_n(\varepsilon - h\nu)]d\varepsilon, \quad (3)$$

$$S_{ss}^{<} \propto \sum_n \int_{-|eV|/2+h\nu}^{|eV|/2} T_n(\varepsilon - h\nu)[1 - T_n(\varepsilon)]d\varepsilon \quad (4)$$

for $V > 0$ and $V < 0$, respectively. As to $\hat{I}_t$, $S_{tt}^{>} = S_{ss}^{<}$ and $S_{tt}^{<} = S_{ss}^{>}$. Because of the charge fluctuations in the C_{60} molecule, the finite frequency noise components S_{ss} and S_{tt} are different. In the zero-frequency limit S_{ss} and S_{tt} yield the standard expression for shot noise [38].

In the weak-coupling, tunneling limit ($T_n \ll 1$) a change of the electrode spacing leads to a mere scaling of the entire transmission function, which results in a nearly constant yield (normalized to 1). As the separation is reduced towards contact, different parts of the transmission spectrum increase at different rates, which reflects the details of the electronic spectrum in the nonequilibrium situation. This behavior may be approximately described with a simplified expression of the yield, for a single channel in the low conductance regime,

$$Y_s^{>} \propto \int_{-|eV|/2+h\nu}^{|eV|/2} \tilde{T}(\varepsilon)d\varepsilon, \quad (5)$$

$$Y_s^{<} \propto \int_{-|eV|/2+h\nu}^{|eV|/2} \tilde{T}(\varepsilon - h\nu)d\varepsilon. \quad (6)$$

Here $\tilde{T} = T/\bar{T}$ is the total transmission T normalized by its average ($\bar{T}$) in the bias window -0.75–0.75 V. The energy dependence of $\tilde{T}$ is shown in Fig. 5 for both polarities. At positive bias, $\tilde{T}$ in the tunneling and contact regimes are rather similar in the energy range 0.45–0.75 eV that is relevant for photon emission. However, for negative bias at contact the transmission $\tilde{T}$ is drastically increased in the emitting energy range (-0.75 to -0.45 eV). This is due to the appearance of HOMO states. At zero and positive bias the HOMO states are filled and do not transmit current. At negative bias and close proximity of the tip and the sample ($G \approx 0.01G_0$), they participate in the current. This results in an enhancement of the fluctuations of charge on the molecule (S_{dd}) and, as a consequence, of the local sample-molecule current (S_{ss}). A similar enhancement is not seen in the molecule-tip current fluctuations (S_{tt}). We thus conclude that the experimentally observed enhancement of photon emission at contact is due to the fluctuations of charge on the molecule (holes in the HOMO states).

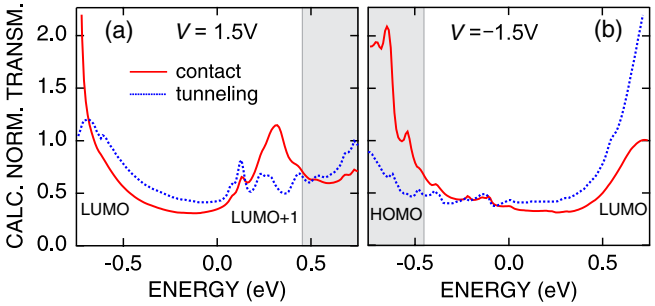

FIG. 5 (color online). Calculated normalized transmission functions $\tilde{T}$ for (a) positive and (b) negative sample voltage V. $\tilde{T} = T/\bar{T}$ is the total transmission T normalized by its average ($\bar{T}$) in the bias window -0.75–0.75 V. The energy ranges that are relevant for photon emission at $h\nu = 1.2$ eV are indicated by gray background.

In summary, we observed that a C_{60} molecule has a drastic effect on the emission of light from a quantum contact. Despite the complexity of the molecular junction the main features of the light emission, its dependence on the conductance and the polarity can be understood in terms of the excess shot-noise properties of the nonequilibrium molecular junction itself. Moreover, we found that the charge fluctuations in the molecule play a major role, and may increase the emission significantly in the contact regime, in contrast to the case of a metal atom contact. The experimental technique and the theoretical approach can provide new insights into the challenging fields of nonequilibrium molecular electronics, quantum noise, and plasmonics.

Financial support by the Deutsche Forschungsgemeinschaft is acknowledged.

[1] A. Nitzan and M. Galperin, Phys. Chem. Chem. Phys. **14**, 9421 (2012).
[2] X. H. Qiu, G. V. Nazin, and W. Ho, Science **299**, 542 (2003).
[3] Z.-C. Dong, X.-L. Guo, A. S. Trifonov, P. S. Dorozhkin, K. Miki, K. Kimura, S. Yokoyama, and S. Mashiko, Phys. Rev. Lett. **92**, 086801 (2004).
[4] E. Cavar, M.-C. Blüm, M. Pivetta, F. Patthey, M. Chergui, and W.-D. Schneider, Phys. Rev. Lett. **95**, 196102 (2005).
[5] T. Uemura, M. Furumoto, T. Nakano, M. Akai-Kasaya, A. Saito, M. Aono, and Y. Kuwahara, Chem. Phys. Lett. **448**, 232 (2007).
[6] C. W. Marquardt, S. Grunder, A. Błaszczyk, S. Dehm, F. Hennrich, H. v. Löhneysen, M. Mayor, and R. Krupke, Nature Nanotech. **5**, 863 (2010).
[7] R. Berndt, R. Gaisch, J. K. Gimzewski, B. Reihl, R. R. Schlittler, W. D. Schneider, and M. Tschudy, Science **262**, 1425 (1993).
[8] G. Hoffmann, L. Libioulle, and R. Berndt, Phys. Rev. B **65**, 212107 (2002).

[9] X. Tao, Z. C. Dong, J. L. Yang, Y. Luo, J. G. Hou, and J. Aizpurua, J. Chem. Phys. **130**, 084706 (2009).
[10] Y. Zhang, X. Tao, H. Y. Gao, Z. C. Dong, J. G. Hou, and T. Okamoto, Phys. Rev. B **79**, 075406 (2009).
[11] N. L. Schneider, F. Matino, G. Schull, S. Gabutti, M. Mayor, and R. Berndt, Phys. Rev. B **84**, 153403 (2011).
[12] G. Schull, N. Néel, P. Johansson, and R. Berndt, Phys. Rev. Lett. **102**, 057401 (2009).
[13] N. L. Schneider, G. Schull, and R. Berndt, Phys. Rev. Lett. **105**, 026601 (2010).
[14] H. E. van den Brom and J. M. van Ruitenbeek, Phys. Rev. Lett. **82**, 1526 (1999).
[15] B. Ludoph and J. M. van Ruitenbeek, Phys. Rev. B **61**, 2273 (2000).
[16] D. Djukic and J. M. van Ruitenbeek, Nano Lett. **6**, 789 (2006).
[17] M. Kiguchi, O. Tal, S. Wohlthat, F. Pauly, M. Krieger, D. Djukic, J. C. Cuevas, and J. M. van Ruitenbeek, Phys. Rev. Lett. **101**, 046801 (2008).
[18] O. Tal, M. Krieger, B. Leerink, and J. M. van Ruitenbeek, Phys. Rev. Lett. **100**, 196804 (2008).
[19] Ya. M. Blanter and M. Büttiker, Phys. Rev. B **59**, 10 217 (1999).
[20] S. S. Safonov, A. K. Savchenko, D. A. Bagrets, O. N. Jouravlev, Y. V. Nazarov, E. H. Linfield, and D. A. Ritchie, Phys. Rev. Lett. **91**, 136801 (2003).
[21] W. Belzig, Phys. Rev. B **71**, 161301 (2005).
[22] Y. Kim, H. Song, D. Kim, T. Lee, and H. Jeong, ACS Nano **4**, 4426 (2010).
[23] A. Nitzan, Annu. Rev. Phys. Chem. **52**, 681 (2001).
[24] G. Hoffmann, J. Kröger, and R. Berndt, Rev. Sci. Instrum. **73**, 305 (2002).
[25] W. W. Pai *et al.*, Phys. Rev. Lett. **104**, 036103 (2010).
[26] G. Schull, T. Frederiksen, M. Brandbyge, and R. Berndt, Phys. Rev. Lett. **103**, 206803 (2009).
[27] G. Schulze *et al.*, Phys. Rev. Lett. **100**, 136801 (2008).
[28] R. Berndt, J. K. Gimzewski, and P. Johansson, Phys. Rev. Lett. **67**, 3796 (1991).
[29] G. Hoffmann, R. Berndt, and P. Johansson, Phys. Rev. Lett. **90**, 046803 (2003).
[30] A. Downes, Ph. Dumas, and M. E. Welland, Appl. Phys. Lett. **81**, 1252 (2002).
[31] J. M. Soler, E. Artacho, J. D. Gale, A. García, J. Junquera, P. Ordejón, and D. Sánchez-Portal, J. Phys. Condens. Matter **14**, 2745 (2002).
[32] M. Brandbyge, J.-L. Mozos, P. Ordejón, J. Taylor, and K. Stokbro, Phys. Rev. B **65**, 165401 (2002).
[33] See Supplemental Material at http://link.aps.org/supplemental/10.1103/PhysRevLett.109.186601 for details of the theoretical derivations and numerical calculations.
[34] U. Gavish, Y. Levinson, and Y. Imry, Phys. Rev. B **62**, R10 637 (2000).
[35] U. Gavish, Y. Levinson, and Y. Imry, Phys. Rev. Lett. **87**, 216807 (2001).
[36] A. V. Lebedev, G. B. Lesovik, and G. Blatter, Phys. Rev. B **81**, 155421 (2010).
[37] P. Johansson, Phys. Rev. B **58**, 10 823 (1998).
[38] Ya. M. Blanter and M. Büttiker, Phys. Rep. **336**, 1 (2000).